Mutual Inductance Extraction and the Dipole Approximation

Rafael Escovar [*] [†] Salvador Ortiz [*] [†] [‡] Roberto Suaya [*]

ABSTRACT

The present work is centered in the controversy between two approaches to inductance extraction: loop vs. partial treatments for IC applications. We advocate for the first one, justifying this claim in terms of representing more realistically the physical situation, as well as having better sparseness properties. We argue that the drawbacks of loop inductance treatment are small for frequencies above 1 GHz. Within the loop inductance formulation, we develop an efficient way of calculating mutual inductances between loops in terms of the field generated by a magnetic dipole. On numerical simulations, the dipole approximation shows good accuracy when compared to FastHenry, down to distances of 30μ for 0.13μ processes. The dipole approximation leads naturally to selection rules for discarding certain couplings that can be experimentally verified.

Categories and Subject Descriptors

J.6 [**Computer Applications**]: COMPUTER-AIDED ENGINEERING—*Computer-aided design (CAD)*

General Terms

Design, Performance, Verification

Keywords

Inductance, Parasitic extraction, Approximation methods, Electromagnetic fields, Mutual coupling

1. INTRODUCTION

Inductance extraction of signal wires is becoming an important concern in Integrated Circuit design as we cross into the GHz frequency range. There are two approaches commonly used to attack the problem of inductance extraction, one based on loop inductance, the other on partial inductance. In this paper, we propose a simplified and computationally efficient way to compute the elements of the inductance matrix M, at all but very short distances, within the loop formalism.

The loop formalism is based on what is known to be the correct physical theory. We start by imposing the correct asymptotic behavior of the magnetic induction field **B** at large distances, which is dominated by the magnetic dipole term. We compute the inductance matrix for a dipole configuration. The resulting expression is computationally inexpensive when compared against analytical models, when the number of participating conductors is larger than two or three. The method is exact for any system provided that we are examining the long distance behavior of the inductance matrix elements. We show that in fact its range of validity extends down to relatively short distances i.e., 30μ for designs at 0.13μ.

The previous result together with some well understood properties of the electromagnetic fields shed some light into the key differences that separate the partial from the loop inductance treatment.

In particular, the differences impact the size of the impedance matrix needed for circuit simulation. It is sparse in the loop inductance formulation, while it is unquestionably dense in the Partial Element Equivalent Circuit (PEEC, [1]) formulation. We examine the source of these differences.

Our approach is based on first principles, and is applicable within the quasi magneto-static domain. We show that the real origin of some of the difficulties associated with the PEEC formulation can be traced to the need for monopoles, in direct conflict with Maxwell's equations.

We present the results of the dipole approximation applied to realistic wire configurations, and make comparisons to the 3D quasi magneto-static field solver FastHenry from MIT [2] and with standard Grover expressions [3]. We develop some simple selection rules for ignoring certain couplings; these rules are exact in the dipole approximation. Their existence is far from evident in the more general formulation. We present some examples and discuss the limits of applicability of the method.

[*]R.Escovar, S.Ortiz, and R.Suaya are with Mentor Graphics Ireland French Branch, 180 Av de l'Europe, 38334 St Ismier, France

[†]S.Ortiz and R.Escovar are Phd candidates at Université Joseph Fourier, Grenoble, France.

[‡]Corresponding author, email: salvador_ortiz@mentor.com

ISPD'04, April 18–21, 2004, Phoenix, Arizona, USA.

2. PARTIAL VS LOOP INDUCTANCE TREATMENTS

To estimate the electromagnetic effects on a multi-conductor system of currents I_i running along loops C_i we consider the associated energy

$$
\begin{aligned}
W &= \frac{1}{2}\sum_i \sum_j W_{ij} \\
W_{ij} &= I_i I_j M_{ij} \qquad (1)
\end{aligned}
$$

where M_{ij} is the i,j element of the inductance matrix. It can be computed from first principles using:

$$
\begin{aligned}
M_{ij} &= \frac{\Psi_{i\to j}}{I_i} \\
&= \frac{1}{I_i}\int_{S_j} \mathbf{B^{(i)}}\cdot \mathbf{dS_j} \\
&= \frac{\mu_0}{4\pi}\left\langle \oint_{C_i}\oint_{C_j} \frac{\mathbf{d\ell_i}\cdot\mathbf{d\ell_j}}{|\mathbf{r_i}-\mathbf{r_j}|}\right\rangle_{\substack{\text{Conductors'}\\ \text{cross-sections}}} \qquad (2)
\end{aligned}
$$

with $\Psi_{i\to j}$ the magnetic flux due to the magnetic induction field, S_j is the surface bounded by C_i, $\mathbf{B^{(i)}}$ generated by the time varying current I_i acting on I_j. In (2) we're assuming the quasi-magneto static regime, whereby the currents I_i, I_j are uniform over the transverse cross sections. The sum in (1) contains as diagonal elements $L_i = M_{ii}$ the self inductance of loop i.

The integrals are evaluated over closed loops, for physical systems, and we speak in this case about loop inductance. The previous equations can be extended to segments [4], giving rise to the PEEC formalism [1], and we speak in this case about partial inductance. On this last formalism, conductor segments are considered to form part of loops closing at infinity.

2.1 Features associated with partial inductance

The partial inductance matrix M has a non physical long distant behavior. In fact, for large wire separation d, its per unit length matrix elements $m_{i,j}$ behave as

$$
m_{ij}(d) \equiv \frac{M_{ij}(d)}{L} \sim -\log(d_{ij}) \qquad (3)
$$

where L is their common length.

The logarithmic decrease with distance manifests itself in two dimensional $2D$ as well as in $3D$ treatments. The only difference between the two cases is the appearance of a constant coefficient $\log(2L)$ in $3D$, which is absent in $2D$. Using Grovers' expressions, the ratio of M_{ij} between a filament i and its closest neighbor j to the corresponding diagonal term L_i has the following limit at large distances (for large d, $d < L$):

$$
\frac{M}{L} \sim 1 - \frac{\log(d/w)}{\log(2L)} \to 1 \qquad (4)
$$

(with w, the wire cross section).

Equations (3) and (4) result in M being dense, and furthermore not diagonally dominant. Matrices of this kind cannot be sparsified by neglecting small non diagonal terms, without incurring in possible passivity violation [5], [6]. Seemingly negligible contributions can affect the sign of the real part of the lowest eigenvalues of M, for an otherwise symmetrical, real and positive definite matrix, simply because it is not diagonally dominant. The system designer is left with two unwanted choices either truncating M and live with passivity violations or live with very large matrices and thereby increase the complexity of downstream circuit simulation.

To investigate the primary source of the denseness, the following statement is useful:

PROPOSITION 1. *The asymptotic behavior* (3) *results from the the following large distance behavior of* $\mathbf{B}$ *:*

$$
\begin{aligned}
B(d) &\sim 1/d^2 \qquad \text{In three dimensions} \\
B(d) &\sim 1/d \qquad \text{In two dimensions} \qquad (5)
\end{aligned}
$$

The above proposition is verified by directly substituting (5) into (2), counting powers in the integrand to estimate the asymptotic behavior, and (3) results.

Proposition 1 springs from:

PROPOSITION 2. *The asymptotic behavior* (5) *results from the presence of unbounded current distributions.*

Consider first the $2D$ case of an infinitely long filament; applying Ampere's law

$$
\oint \mathbf{B}\cdot\mathbf{dl} = \mu_0 I \qquad (6)
$$

and extracting B

$$
\begin{aligned}
B(d) &= \frac{\mu_0 I}{2\pi d} \\
m(d) &= \frac{\int B\,\mathrm{d}d}{I} = \frac{\mu_0}{2\pi}\log(\frac{d}{w}) \qquad (7)
\end{aligned}
$$

which gives precisely (3).

In $3D$, start from the vector potential $\mathbf{A}$

$$
\mathbf{A}(\mathbf{r}) = \frac{\mu_0}{4\pi}\int_V \frac{\mathbf{J}(\mathbf{r}')}{|\mathbf{r}-\mathbf{r}'|}\mathrm{d}^3 r' \qquad (8)
$$

and carry out, as in [7], a multi-pole expansion of the Green Function $1/|\mathbf{r}-\mathbf{r}'| = 1/|\mathbf{r}+\mathbf{r}\cdot\mathbf{r}'/|\mathbf{r}|^3 + ...$, giving :

$$
A_i(\mathbf{r}) = \frac{\mu_0}{4\pi}\left(\frac{1}{|\mathbf{r}|}\int_V J_i(\mathbf{r}')\mathrm{d}^3 r' + \frac{\mathbf{r}}{|\mathbf{r}|^3}\cdot\int_V \mathbf{r}' J_i(\mathbf{r}')\mathrm{d}^3 r' + \ldots\right) \qquad (9)
$$

For $B(d) \approx 1/d^2$ as demanded by (3), the first term in (9) must be different from zero. It is on the other hand well known that for any bounded current distribution in the quasi-static regime $\partial\rho/\partial t = 0$, with ρ the charge density, the integral in the first term of (9) vanishes (the volume V of integration includes the entire current distribution). Thus, under quasi-static conditions and for bounded current distributions, $\mathbf{A}$ must fall off for large distances at least as rapidly as $1/r^2$. Using $\mathbf{B} = \nabla\times\mathbf{A}$ we conclude that for bounded physical systems:

$$
\mathbf{B} \sim 1/r^3, \qquad (10)
$$

equations (3) and (5) are invalid and m falls down with distance as a power law. The PEEC method is in violation with the asymptotic behavior of Maxwell's equations. Dropping the assumption of bounded current distributions is tantamount to the presence of monopoles in the theory, whereas dropping the quasi static assumption requires a completely new approach.

The previous are rigorous results in Electromagnetism. A current loop treatment of quasi-magneto-static loop inductance must therefore necessarily give rise to a significantly more localized magnetic influence than what would be resulting from the PEEC approach.

2.2 Sparsification

There has been widespread work to improve on the PEEC formalism ([8, 9] and references therein). The underlying goal is to sparsify the dense M matrix while preserving its positive definiteness.

The behavior (5) of magnetic fields within a partial inductance treatment(magnetic field produced by a magnetic monopole) is formally equivalent to that of the electrical field produced by a point charge.

This similarity has inspired some researchers to explore the notion of inverse methods [8, 10]. In few words, these consist of first inverting locally the M matrix, and then sparsifying the $K \equiv M^{-1}$ matrix. The analogy clearly extends to C and K which play similar roles in the electrostatic and magneto-static problems, respectively ($Q = C\Delta V$, $j\omega I = K\Delta V$).

However, there is an important difference between the two cases: for the C matrix, the local truncation prior to inversion is well justified, due to the fact that C, in the Maxwell sense, is diagonal dominant by construction, and thus any truncation preserves positive definiteness; on the other hand the jury is still out regarding the diagonal dominance of K [11].

At variance with C, the matrix K is not physical, and it is not obvious how to extend the concept of shielding, present in the electrostatic case. Shielding of electrical fields by conductors, cause the **E** field to be localized in a dense wire environment, making the C matrix sparse. In the magneto-quasi-static case there is no physical equivalent shielding, currents and the **B** field fully penetrate the conductors. Nonetheless, it is empirically verified that K is sparse,yielding a considerable amount of strength to partial inductance followed by inverse methods. A loop inductance method, on the other hand, has inherent localization properties deriving from (10), as we shall derive on (28) while preserving the correct physical theory.

3. RETURN PATH IN THE LOOP INDUCTANCE FORMULATION

Partial inductance methods do not require *a priori* identification of the return paths followed by currents along signal wires. The contrary happens in the loop inductance formulation.

We proceed to show that large uncertainties related to the problem of return path selection do exist, but are mainly limited to low frequencies, where in fact inductance effects are unimportant.

For this purpose, we define the concept of *bundle*, as the set of parallel wires of equal length consisting of one signal plus all its possible return paths. We regard a bundle as a set of closed loops with one common segment (namely the signal wire), neglecting the absence of the small segments in the orthogonal direction needed to close the loops.

In this section, we show some practical rules for constructing these bundles, as well as for calculating the values R_{Loop} and L_{Loop}, i.e. the resistance and self inductance for bundles. In other words, we are now computing the diagonal elements of the impedance matrix,

$$Z(\omega) = R + j\omega L, \tag{11}$$

The return path, at any frequency, is the one that minimizes Z. At low ω, this corresponds to resistance R minimization, while for large ω it demands inductance L minimization.

Let us consider a representative case for illustration: a *Cu* wiring used for clock signal routing at 0.13μ CMOS processes. The loop inductance per unit length $l = O(10^{-7} H/m)$ while the loop resistance per unit length $r = O(5000\Omega/m)$ We can characterize four distinct frequency regimes, namely:

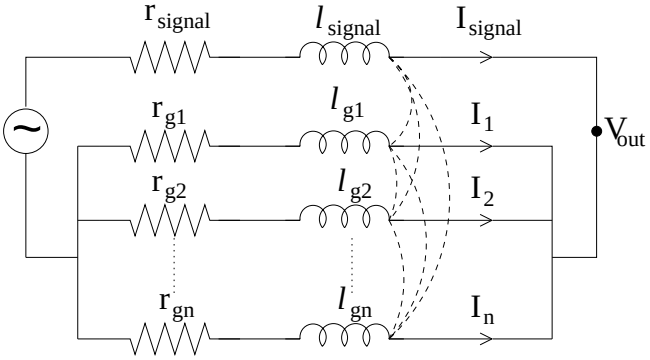

Figure 1: Circuit equivalence of a bundle with n return paths (for simplicity, mutual inductances between wires are depicted as dashed lines without label).

1. Low frequencies, $r \gg \omega l$ ($f < 1GHz$ in our example.)
2. Intermediate frequencies, $r \geq l\omega$ ($f < 8GHz$ in our example)
3. Large frequencies $r < l\omega$, while current distribution within conductors is still uniform. ($8GHz \leq f \leq 15GHz$ for our example)
4. Very large frequencies $r \ll l\omega$. Non uniform current distributions. ($f > 15GHz$ in our example).

At present, on CMOS technologies we need to contend with the first two regimes and an emerging third regime. (Maximum frequency content of a signal at 0.13μ is dictated by circuit considerations and is approximately $10GHz$.)

Regimes 1 and 2 are resistance dominated. In what follows we discuss the self loop inductance for regimes 1 to 3.

We consider a wire configuration consisting of a signal wire and its (not necessarily coplanar) return paths. We are interested in calculating the currents I_i running along return path i when a unit amplitude voltage source is connected between the signal and the n return wires of the bundle (see Fig.1). This can be done with elementary circuit analysis. We have

$$\Delta V = ZI \tag{12}$$

where

$$\Delta V = \begin{pmatrix} 1 - V_{out} \\ -V_{out} \\ \vdots \\ -V_{out} \end{pmatrix}, \; I = \begin{pmatrix} I_{signal} \\ I_1 \\ \vdots \\ I_n \end{pmatrix}, \text{ such that } \sum_{i=0}^{n} I_i = 0$$

These currents I_i give the (complex) weight of each return path within each bundle. Normalized by the current I_{signal}, their sum is unity. We define the values α_i

$$\alpha_i \equiv I_i / I_{signal} \tag{13}$$

analogous but more general than [12].

Solving (12) can be computationally expensive when there is a large number of return paths in a bundle, since it involves computing the inverse of an $(n+1) \times (n+1)$ matrix. A large number of return paths are only needed in Regime 1, in which currents can

go far away to find low resistive paths. But in this regime, we follow [12], neglecting the inductance component in the calculation of I_i, and then computing the inductance based on these currents. Thus for Regime 1, we have $I_i \propto R_i^{-1}$ and the resulting expressions are:

$$\begin{aligned} R_{loop} &= R_0 + R_g \\ &\quad \text{where} \quad \mathrm{R_g^{-1}} = \sum_{\mathrm{i=1}}^{\mathrm{n}} \mathrm{R_i^{-1}} \\ L_{loop} &= \sum_{i=0}^{n} \alpha_i \sum_{k=0}^{n} \alpha_k M_{ik} \\ &\quad \text{where} \quad \alpha_0 \equiv 1,\ \alpha_\mathrm{i} \equiv -\frac{\mathrm{R_g}}{\mathrm{R_i}}\ \forall \mathrm{i} > 0 \end{aligned} \qquad (14)$$

For a signal wire in regime 1, the dominant term R_{loop}, is minimized by including all parallel ground wires ordered by their resistance. The distance between signal and ground(s) plays no role. Far away return wires contribute to make the overall inductance large. The impact on Z is small, since ω is small in regime 1. This balance explains the large possible spread of return path choices. For a signal in regime 2, where both contributions are of the same order of magnitude, while r dominates, the choice of return path is a balance in between minimizing R_g and minimizing L and therefore the length of the overall path, and d. A good compromise is obtained by including as return path wires organized according to resistance, up to a maximum distance that is problem dependent. For signals in regime 3, inductance is much more important, meaning that the modulus of the α_i computed in (13) will be larger for those wires having larger inductance. Inductance being dominant, to minimize the loop integral in (2) the return path is localized around the closest ground neighbors. Finally for signals in the regime 4, resistance does not matter, any close neighbor ground or signal can act as a valid return path. Since the number of close near neighbors is small, full inversion methods to compute α_i are appropriate.

The mechanism proposed above leads naturally to the explanation of one salient property of the proximity effect. Loop self inductance, in the regime of uniform current distribution decreases with frequency in going from regions 1 to 3, due to the change of return path being selected. In regime 4, where currents cease to be uniform, there are other manifestations of proximity effect, associated with the skin effect, which are not considered here. From this discussion we conclude, that except for signals in region 1, where inductance does not matter, it is relatively uncomplicated to select return path configurations from a pool of ground wires. The use of the physically rigorous method of loop inductance becomes for these cases reasonable and expedient.

The scope of the present work is principally regimes 1,2 and eventually 3, where there is a fair amount of wires per bundles and thus a simplification is worthy.

It should be obvious that in employing a loop inductance method, a reduction in size of the underlying system is obtained. Namely, this reduction consists in having an equivalent circuit representation in which several resistances and inductances collapse into one (see [13]).

4. MUTUAL INDUCTANCE, DIPOLE APPROXIMATION

We now develop a method to compute the *mutual inductance between bundles* M_{ab}, i.e. the off-diagonal terms in the Z matrix. Thus the aim is to arrive at an expression analogous to (1), but for bundles, $M_{ab} = W_{ab}/(I_a I_b)$, with currents I_a(resp. I_b), running

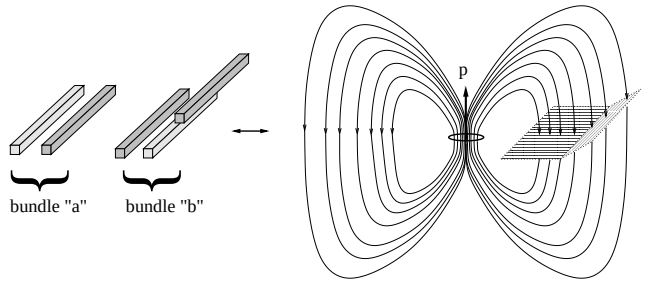

Figure 2: Schematic view of the dipole approximation for calculating the interaction between two bundles.

along the signal wires of bundle $a(b)$. For this purpose we begin precisely from (1), with subindex $i(j)$ sweeping all wires in bundle $a(b)$.

As in the previous section, the current I_b is divided among the return paths according to the coefficients α_j,

$$I_j = \alpha_j I_b \qquad \text{with } \alpha_0 = 1,\ \sum_{j\geq 1} \alpha_j = -1 \qquad (15)$$

Consequently, W_{ab} in (1) can be factored as

$$W_{ab} = \frac{I_b}{2} \sum_{j\geq 1} \alpha_j \Psi_{a\to j} \qquad (16)$$

Here $\Psi_{a\to j}$ is the magnetic flux of all wires in bundle a through the surface of elementary closed loop S_j of bundle b (see Fig.2)[1]

These fluxes are computed using Stokes' theorem,

$$\Psi_{a\to j} = \iint_{S_j} (\nabla \times \mathbf{A^{(a)}}) \cdot \mathbf{dS_j} = \oint_{\partial S_j} \mathbf{A^{(a)}} \cdot \mathbf{d\ell_j} \qquad (17)$$

with $\mathbf{A^{(a)}}$ the vector potential due to all wires in bundle a, and ∂S_j is the boundary of surface S_j. By definition, this curve is formed by the union of the signal wire and the return path j, each with the proper sign. Summing up all the terms, expression (16) becomes

$$W_{ab} = \frac{I_b}{2} \sum_{j\geq 0} |\alpha_j| \int_{C_j} \mathbf{A^{(a)}} \cdot \mathbf{d\ell_j} \qquad (18)$$

where C_j is the conductor $j \geq 0$.

Next we take into account the magnetic dipole approximation, whereby we consider the field due to all the circuits in bundle a as the one generated by a representative dipole moment $\mathbf{p_a}$ [7].

To compute the value of $\mathbf{p_a}$, we first consider the dipole of a configuration of two parallel wires lying on the $x-y$ plane, one being the return path of the other (Fig.3a). In this simple case,

$$\begin{aligned} \mathbf{p_a} &= \frac{\mu_0}{8\pi} \int \mathbf{r} \times \mathbf{J}(\mathbf{r}) \mathrm{d^3 r} \\ &= \frac{\mu_0}{8\pi} ILs\hat{z} \end{aligned} \qquad (19)$$

[1] In doing this, we neglect the fact that these pairs in bundle b are not really closed, since they are missing the perpendicular segments at the ends; the error committed is small as long as the transverse dimensions, i.e. the lengths of these segments, are small compared to the length of the bundle and the separation between bundles.

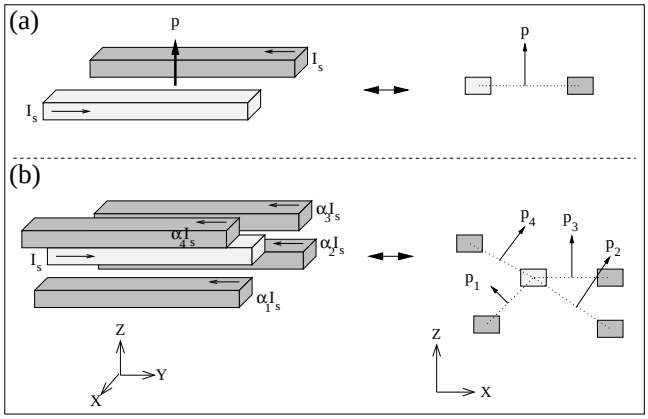

Figure 3: Calculation of dipole moment for a bundle: (a) simple case with one unique return path; (b) bundle with several return paths, where the resulting p is a weighted average of all the $\mathbf{p}_i$.

where L is the common length of the two wires and s is the separation between them (p_a is proportional to the area spanned by the circuit and points in the direction $\hat{z}$ perpendicular to the plane containing them.)

For bundles having multiple return paths (all oriented along the y axis, see Fig.3b), the integral in the first line of (19) is decomposed into several terms like the one in the second line. Since each of those terms is proportional to the current it carries, they are weighed again by geometrical coefficients $\alpha_i,\ i \in a$ as in (16).

Therefore the expression for the magnetic moment becomes,

$$\mathbf{p_a} = \frac{\mu_0}{8\pi} I_a \sum_{i\geq 0} \alpha_i (\hat{y} \times \mathbf{r_i}) \tag{20}$$

where $\mathbf{r_i}$ is the position of return path i with respect to the signal wire.

Since the total current in a bundle adds up to zero, the value obtained by (20) is independent of where the origin of coordinates is located. We choose this origin as the position of the "center of mass" of bundle a,

$$\mathbf{r_{cm,a}} = \frac{1}{2} \sum_{i\geq 1} \alpha_i \mathbf{r_i} \tag{21}$$

i.e., as the weighted average of the position of all the constituent moments of the form (19).

The expression for the vector potential $\mathbf{A}$ at position $\mathbf{r}$ due to a dipole $\mathbf{p_a}$ at the origin is

$$\mathbf{A}^{(\mathbf{a})} = \frac{\mathbf{p_a} \times \mathbf{r}}{r^3} \tag{22}$$

The $1/r^2$ behavior of $\mathbf{A}$ corresponds to the $1/r^3$ behavior for $\mathbf{B}$ as demanded by (10).

Replacing expression (22) into (18), we arrive at a closed expression of the mutual inductance between bundles M_{ab}, within the dipole approximation,

$$M_{ab} = \frac{1}{I_a} \sum_{j\geq 0} |\alpha_j| \int_{C_j} \frac{(\mathbf{p_a} \times \mathbf{r_j})}{r_j^3} \cdot \mathbf{d}\ell_j \tag{23}$$

Inspection of (20) and (23) shows that $\mathbf{p_a}$ is proportional to I_a; hence, M_{ab} does not depend on the currents, but is solely a geometric coefficient, as should be expected. For the sake of notation, from here on, we use $\tilde{\mathbf{p}}_\mathbf{a}$ to stand for $\mathbf{p_a}/I_a$.

As mentioned before, all conductors in a bundle run along the same direction, say $\hat{y}$. Thus $\mathbf{p_a}$ is perpendicular to all the wires. We have the freedom to choose the $\hat{z}$ axis parallel to the dipole moment $\mathbf{p_a}$, and (23) becomes

$$M_{ab} = \tilde{p}_a \sum_{j\geq 0} |\alpha_j| x_j \int_{y_{0,j}}^{y_{1,j}} \frac{\mathrm{d}y}{(x_j^2 + y_j^2 + z_j^2)^{3/2}} \tag{24}$$

where $y_{0,j}$ and $y_{1,j}$ are the extremes of conductor j, in a coordinate system with origin at $\mathbf{r_{cm,a}}$. Expression (24) is effortlessly integrated,

$$M_{ab} = \tilde{p}_a \sum_{j\geq 0} \frac{|\alpha_j| x_j y_j}{(x_j^2 + z_j^2)(x_j^2 + y_j^2 + z_j^2)^{1/2}} \Bigg|_{y_j = y_{0,j}}^{y_j = y_{1,j}} \tag{25}$$

Thus mutual inductance between two bundles is reduced to calculating the dipole moment and the position of the first bundle via (20) and (21), and then evaluating the simple expression (25) for each of the wires of the second bundle.

Similarly, we can construct the expression for $\mathbf{p_a}$ for wires layout along the x-axis.

In order to compare with classical Grover expressions, this last expression would replace the one arising from the combination of filament-to-filament interactions [3],

$$M_{ab} = \frac{\mu_0 L}{4\pi} \sum_{i\geq 0} \sum_{j\geq 0} \alpha_i \alpha_j M_{ij} \tag{26}$$

$$\text{where} \quad M_{ij} = \log\left(\frac{L}{d_{ij}} + \sqrt{1 + \frac{L^2}{d_{ij}^2}} \right) + \frac{d_{ij}}{L} - \sqrt{1 + \frac{d_{ij}^2}{L^2}}$$

For example, in a very simple configuration like the one shown in Fig. 4a it is straightforward to see that both expression (25) and (26), for $x, L \gg s_1, s_2$, give exactly the same limit, namely

$$M_{ab} \simeq \frac{\mu_0}{4\pi} s_1 s_2 L_1 L_2 \frac{2x^2 + L_2^2/4}{x^2 (x^2 + L_2^2)^{3/2}} \tag{27}$$

As anticipated in section II, once all terms are accounted for, in the loop inductance treatment, the asymptotic behavior of M is quite unlike that of (3). In fact, (27) shows two types of regimes for transverse coupling (we take $s_1 = s_2 \equiv s$ and $L_1 = L_2 \equiv L$ for simplicity),

$$M_{ab} \simeq \begin{cases} \frac{\mu_0}{2\pi} \frac{s^2 L^2}{x^3} & \sim \frac{1}{d^3} \quad \text{for } x \gg L \text{ (3d case)} \\ \frac{\mu_0}{16\pi} \frac{s^2 L}{x^2} & \sim \frac{1}{d^2} \quad \text{for } x \ll L \text{ (2d case)} \end{cases} \tag{28}$$

In a case of forward coupling, like the one shown in Fig.4b, the comparison with the Grover expressions, now in the limit $L_1, L_2, \Delta_y \gg s_1 = s_2 \equiv s$, gives

$$\begin{aligned} M_{ab}^{\text{dipoles}} &\simeq \frac{2\mu_0}{\pi} \frac{s^2 L_1 L_2 \Delta_y}{(4\Delta_y^2 - L_2^2)^2} \\ M_{ab}^{\text{grover}} &\simeq \frac{\mu_0}{2\pi} \frac{s^2 L_1 L_2 \Delta_y}{(4\Delta_y^2 - L_1^2 - L_2^2)^2 - (2L_1 L_2)^2} \end{aligned} \tag{29}$$

both expressions having the same asymptotic behavior.

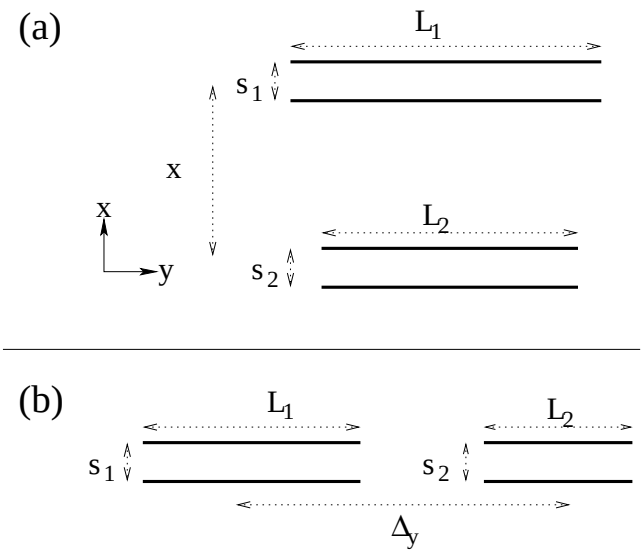

Figure 4: Simple configurations for the sake of comparison or (25) **with Grover's expressions:(a) transverse coupling; (b) forward coupling.**

5. RESULTS

In this section, we study the regime of validity of the dipole approximation. We do this by comparison between (25) with the results obtained with the field solver FastHenry [2].

It is self evident that calculating the mutual inductance using the dipole approximation is considerably less expensive computationally than FastHenry. All the simulations in FastHenry were carried out at a frequency of 10GHz. To assure good convergence with FastHenry, we empirically found that 9×9 filament partitioning suffices. In some cases, 5×5 was accurate enough.

The dipole approximation is also less expensive than the direct use of Grover's expressions (26). An analysis of the performance is included at the end of the present section.

All calculations using the dipole approximation used coefficients α_i based solely on resistance, as in [12] (see Section 3).

A good criterion to be used in considering the errors introduced in a mutual inductance extraction method is the comparison to the (always larger) self inductances of the two bundles, L_a, L_b. For this reason, we choose to plot the dimensionless magnitude $\zeta \equiv M_{ab}/\sqrt{L_a L_b}$.

5.1 Numerical comparisons with FastHenry

First, we show in Fig.5 the simplest case, with both bundles consisting of one signal wire and a single return path. Notice that the relative position between signal and return is perpendicular in one bundle with respect to the other. From the results displayed in this figure, we can state that the dipole approximation shows relative discrepancies with FastHenry which are at most 10%. Considering that mutual inductance, in this case, is two or three orders of magnitude smaller than the self inductances, this means that the error introduced by this approximation is, at worst, in the third significant digit.

We consider next two bundles with one return path each, but in this case their dipole moments are parallel (see Fig.6). Again, the resulting comparison with FastHenry also show discrepancies upper bounded by 10%. We may conclude that the dipole approximation holds then very well for mutual inductances between bundles

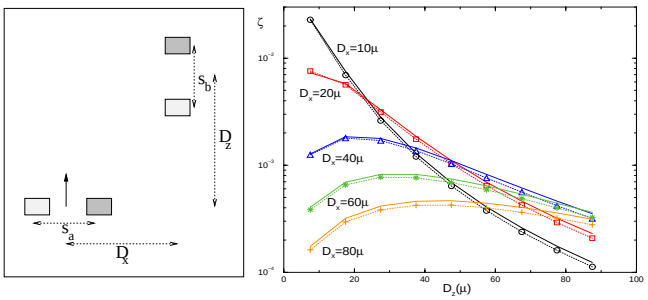

Figure 5: Comparison between the dipole approximation (solid lines) and FastHenry (dotted lines with symbols) for perpendicular bundles, geometries like the one shown at right, plotted for different values of D_x as a function of D_z. Values not shown are: $L = 500\mu, s_a = s_b = 5\mu$ and $h = 0.1\mu, w = 0.1\mu$ for all conductors.

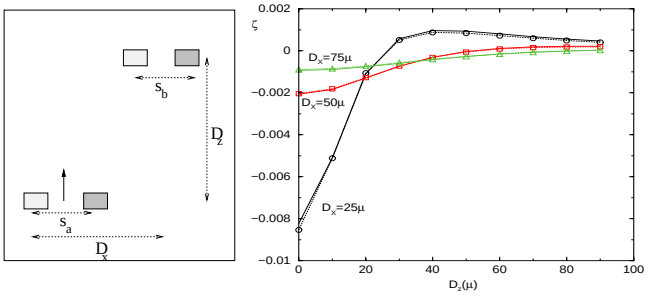

Figure 6: Comparison between the dipole approximation (solid lines) and FastHenry (dotted lines with symbols) for parallel bundles, geometries like the one shown at right, plotted for different values of D_x as a function of D_z . Values not shown are: $L = 500\mu, s_a = s_b = 5\mu$ and $h = 0.1\mu, w = 0.1\mu$ for all conductors.

with single return path each, irrespective of the orientation of their dipole moments.

We next show a slightly more complicated geometry, consisting of two bundles with multiple return paths each. Both are asymmetric, in the widths of the return paths as well as in their positions with respect to the signal wire (see Fig.7).

In this example, we find that for the case of the closest configurations ($D_x = 15\mu, D_z \leq 20\mu$) there is a considerable difference between the two results. It should be noted, however, that even in those cases, the value of K is very small, thus rendering the aforementioned errors insignificant when compared to the self inductances L_a, L_b.

In few words, these examples are indicative of a general tendency that holds for arbitrary configurations: as long as distance between bundles is not too narrow ($\sim 30\mu$), the leading dipole representation gives a fairly good approximation for the mutual inductance.

5.2 Dipole selection rules

As can be seen by deeper analysis, there are a a fair number of situation-dependent rules that hold. They are of importance in the action of pruning unnecessary couplings.

1. For perfectly symmetric bundles, the mutual inductance is null.

2. For two parallel bundles (e.g. Fig.8), the mutual inductance between them is minimized when their relative position forms

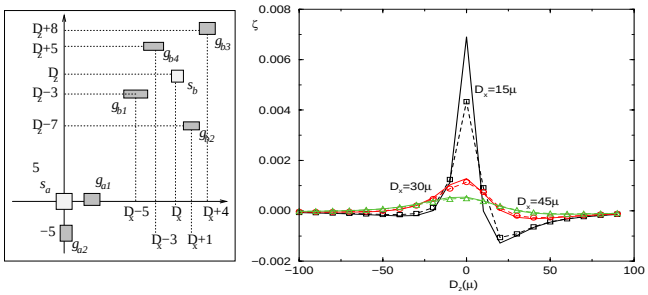

Figure 7: Comparison between the dipole approximation (solid lines) and FastHenry (dotted lines with symbols) for a more complete geometry, as shown at right. The widths of the wires are: $w_{s_a} = 0.1\mu, w_{s_b} = 0.1\mu, w_{g_{a1}} = 0.2\mu, w_{g_{a2}} = 0.3\mu, w_{g_{b1}} = 0.3\mu, w_{g_{b2}} = 0.2\mu, w_{g_{b3}} = 0.1\mu, w_{g_{b4}} = 0.15\mu$**. Other values are:** $L = 500\mu$, **and** $h = 0.1\mu$ **for all conductors.**

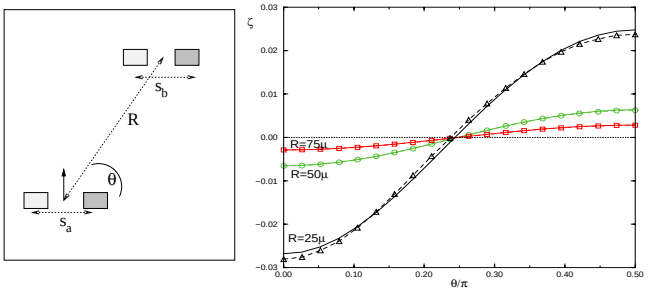

Figure 8: Selection Rule 2, showing the angular dependence of mutual inductance for different separation between bundles: dipole approximation (solid lines) and FastHenry (dotted lines with symbols)

a certain angle with the common direction of their dipole moments; the value of this angle goes from 45° when the bundles are much longer than the transverse dimensions, to $\sim 35°$ when this is not the case.

3. For two perpendicular bundles (e.g. Fig.5), mutual inductance is negligible for situations where one is near the vertical axis passing through the center of the other.

An example configuration of the first selection rule is given by a sandwich configuration. (i.e., a perfectly symmetric coplanar ground-signal-ground bundle). It has zero dipole moment, meaning that in the dipole approximation its signal voltage is insensitive to external noise. Verification of this rule with FastHenry, calculating the mutual inductance between two of these structures, gives values of ζ below 10^{-5} even for separation between bundles as low as 5μ. This result has important consequences on the stability of clock signal lines [13].

Regarding the second rule, we exemplify, for the sake of simplicity, with bundles consisting of one return path each. For the case of long bundles, this rule can easily be deduced from Taylor expansion of (25) under the conditions $s \ll x, z \ll L$. Doing so, it is seen that M_{ab} exactly vanishes when $x = z$, i.e. when $\theta = 45°$. In the case of short bundles, this rule springs from the expression for the perpendicular component $B_\perp$ for the field of a dipole (30), which is null for $\theta = 0.5\cos^{-1}(1/3) \approx 35°$. Numerical examples for this situation are shown in Fig.8. This rule can be considered an important criterion for designers wishing to minimize mutual inductance.

$$\begin{aligned} \mathbf{B}(\mathbf{r}) &= \frac{3(\mathbf{p}\cdot\hat{\mathbf{r}})\hat{\mathbf{r}} - \mathbf{p}}{r^3} \\ B_\perp &= \frac{1}{2}(3\cos 2\theta + 1)\frac{p}{r^3} \\ B_\parallel &= \frac{3}{2}\sin 2\theta \frac{p}{r^3} \end{aligned} \qquad (30)$$

As to the third rule, it is a consequence of the fact that the parallel component $B_\parallel$ for the field of a dipole vanishes at $\theta = 0$ and $\theta = 90°$. In one of the examples shown previously (Fig.5) this situation manifests itself in two aspects: (a) the drop in mutual inductance for small values of D_z; (b) for D_z large, ζ decreases with decreasing D_x. This rule is very useful for pruning large layouts.

5.3 Performance analysis

In order to analyze the efficiency of the present dipole approximation, we compare its runtimes with respect to the direct use of Grover's expressions (26). We mention briefly that these last expressions give basically the same results as FastHenry, meaning that the errors between the dipole approximation and Grover's expressions are as small as the ones presented in the previous sections.

If we consider a general case, with N wires broken up into n_b bundles, Grover's expressions require $N^2/2$ computations of terms as in the second line of (26). On the other hand, the dipole approximation requires a total of $n_b N$ calculations. Thus, if there are on average considerably more than one return path per bundles (ie, if $n_b \ll N/2$), then the dipole approximation implies a much smaller number of evaluations. Moreover, each of the evaluations of Grover's expression involves a transcendental function, whereas for the dipole approximation there are N evaluations arising from the calculation of dipole moment, which are only sums and multiplications (see eq.(20)), plus $(n_b - 1)N$ evaluations as in the argument in the sum of (25), where the most expensive operation is a half-power.

Table 1: Comparative runtimes for Dipole approximation (DA) and Grover's expressions (GE) as a function of the number of return paths N; times expressed in microseconds per evaluation

N	DA	GE	Ratio GE/DA
1	0.412	1.586	3.85
2	0.544	3.343	6.14
3	0.697	5.817	8.34
4	0.784	9.052	11.54
5	1.000	13.002	13.00
6	1.092	17.902	16.39

In Table 1 we present a comparison between the two methods for concrete examples involving two bundles with the same number of return paths in each one. Runtimes are expressed in microseconds per mutual inductance computation ($\sim 10^8$ similar computations are averaged for each entry of the table). All runs were carried out on a desktop PC running at 2.0 GHz, under identical situations. The approximately linear increase of the runtime ratios with bundle size (last column of Table 1) shows that, at least in this case, the dipole approximation is one order of magnitude faster than the use of Grover's expressions.

6. CONCLUSIONS

We claim to have contributed to the understanding and simplification on the problem of mutual inductance computations relevant in IC design, in terms of simple dipole structures. For distances that are not too close the dipole representation computes with good precision the behavior of the mutual inductance matrix. When the physical loops are seen in terms of dipoles, it is easier to separate what is important from what is negligible. The resulting selection rules emerge quite naturally, and further contribute to the sparsification. Considering an inductance matrix that falls as $1/d^2$ or $1/d^3$ makes the problem of bounding the size of the extraction matrix manageable. This feature simplifies enormously the effort during downstream circuit simulation. Previous work [14] have attributed to small current loops the term dipoles, without further ado. FastHenry used effectively the multi-pole expansion of the electrostatic Green Function in their field solver. Our analysis goes beyond in providing a framework for the proper extraction of the mutual inductance matrix for a wide range of distances. At very small distances, where the dipole approximation is no longer applicable, we simply need to compute the loop mutual inductances in terms of the algebraic sum of Grover like expressions. Since our approach relies on measurable quantities it is feasible to ratify or rectify experimentally by simply verifying for example some of the selection rules or the inverse power like behavior.

7. REFERENCES

[1] A. E. Ruehli, "Inductance calculations in a complex circuit environment," *IBM J.Res.Develop.*, vol. 16, pp. 470–481, 1972.

[2] M. Kamon, M. J. Tsuk, and J. White, "Fasthenry: A multipole-accelerated 3-d inductance extraction program," *IEEE Trans. Microwave Theory Tech.*, vol. 42, no. 9, pp. 1750–1758, Sept. 1994.

[3] F. Grover, *Inductance Calculations Working Formula and Tables*. New York: Instrument Society of America, 1945.

[4] E. Rosa, "The self and mutual inductance of linear conductors," *Bulletin of the National Bureau of Standards*, vol. 4, pp. 301–344, 1908.

[5] G. Golub and C. van Loan, *Matrix Computations, 3rd Ed.* Baltimore: The Johns Hopkins University Press, 1992.

[6] M. Beattie, B. Krauter, L. Alatan, and L. Pileggi, "Equipotential shells for efficient inductance extraction," *IEEE Trans. CAD of IC and Systems*, vol. 20, pp. 70–79, 2001.

[7] J. Jackson, *Classical Electrodynamics*. New York: John Wiley and Sons, Inc., 1962.

[8] A. Devgan, H. Lin, and W. Dai, "Hot to efficiently capture on-chip inductance effects: Introducing a new circuit element *k*," in *Computer Aided Design, IEEE/ACM International Conference on*, Nov 2000, pp. 150–155.

[9] M. Beattie and L. Pileggi, "Inductance 101: Modeling and extraction," *Design Automation Conference*, pp. 323–328, 2001.

[10] ——, "Efficient inductance extraction via windowing," *Proc.Design,Automation, and Test in Europe*, pp. 430–436, 2001.

[11] C. Tsung-Hao Chen, C.Luk, "INDUCTWISE: inductance-wise interconnect simulator and extractor," in *Computer-Aided Design of Integrated Circuits and Systems, IEEE Transactions on*, vol. 22, no. 7, 2003, pp. 884–894.

[12] B. Krauter and S. Mehrotra, "Layout based frequency dependent inductance and resistance extraction for on-chip interconnect timing analysis," in *Proc. 35th ACM/IEEE DAC*, Jan. 1998, pp. 303–308.

[13] R. Escovar and R. Suaya, "Transmission line design of clock trees," in *Proc. IEEE/ACM International Conference on CAD*, Nov. 2002, pp. 334–340.

[14] T. Lin, M. Beattie, and L. Pileggi, "On the efficiency of simplified 2d on-chip inductance models," in *Design Automation Conference*, 2002, pp. 757–762.